Supporting Information

Mechanism, Selectivity, and What Prevents Closure of the Catalytic Cycle for H_2 Reduction of CO_2 Promoted by a Heterodinuclear Zirconium-Iridium Complex

Kevin P. Quirion[a] and Daniel H. Ess*[a]

[a] Department of Chemistry and Biochemistry, Brigham Young University, Provo, UT 84604, USA

Table of Contents

Computational Methods

Nudged elastic band (NEB) scans were performed using the ORCA 6.0[1] software with the B3LYP-D3[2] functional and the def2-SVP[3] basis set. This was done with the intermediates **3a**, **3b**, **3 + H_2**, **4a** and **4c** obtained from previous Gaussian 16[4] optimizations at the B3LYP-D3/SDD-6-31G(d)/gas[5] level of theory without further optimization. All energies obtained were electronic energies in kcal/mol.

B3LYP-D3 Energies with Thermal Corrections, M06 Energies, and Coupled Cluster Energies

Table S1. Computed energies and imaginary frequencies of optimized structures.

Complex[a]	SCF	ZPE	Enthalpy	Free energy	SP-Free energy[b]	DLPNO-CCSD(T)[c]	Freq.
CO_2	-188.577760	-188.566146	-188.562562	-188.587517	-188.558667	-188.332064	-
H_2	-1.175482	-1.165337	-1.162033	-1.176825	-1.170085	-1.167997	-
PhLi	-239.138958	-239.049581	-239.042741	-239.079153	-239.028472	-238.664604	-
1	-1141.422757	-1140.903029	-1140.870102	-1140.966921	-1140.781938	-1138.823828	-
2	-1142.621586	-1142.084196	-1142.051439	-1142.146208	-1141.973140	-1140.022329	-
2'	-1142.619730	-1142.082527	-1142.049351	-1142.143765	-1141.972942	-	-
2a	-1142.569572	-1142.036084	-1142.002503	-1142.097397	-1141.927951	-	-
3	-1330.041918	-1329.506048	-1329.471317	-1329.568244	-1329.359186	-1327.193272	-
3'	-1330.000077	-1329.465222	-1329.430357	-1329.527674	-1329.316715	-	-
4a	-1331.242254	-1330.686967	-1330.650878	-1330.751380	-1330.556748	-1328.385208	-
4b	-1331.249438	-1330.694074	-1330.658126	-1330.759308	-1330.563244	-1328.392033	-
4c	-1331.194209	-1330.636808	-1330.60032	-1330.701776	-1330.515685	-	-
5	-196.757813	-196.733710	-196.728894	-196.759110	-196.737065	-196.489122	-
6	-189.752912	-189.719021	-189.714922	-189.743104	-189.731229	-189.504574	-
7	-1373.677390	-1373.054845	-1373.017468	-1373.119950	-1372.894711	-1370.632349	-
7'	-1373.631898	-1373.010332	-1372.972397	-1373.076130	-1372.847723	-	-
TS1a	-1330.004349	-1329.470192	-1329.435052	-1329.532882	-1329.330539	-1327.147922	-120.58
TS1b	-1142.597193	-1142.062973	-1142.029322	-1142.125233	-1141.954312	-1139.989583	-181.05
TS1c	-1142.569572	-1142.036084	-1142.002503	-1142.097397	-1141.927951	-1139.960968	-502.50

TS2	-1331.209023	-1330.658860	-1330.623018	-1330.724452	-1330.530124	-1328.348313	-269.61
TS2a	-1331.190661	-1330.640831	-1330.605237	-1330.704532	-1330.498787	-	-778.76
TS2b	-1331.163595	-1330.614686	-1330.578617	-1330.679027	-1330.481530	-	-520.80
TS2c	-1331.159311	-1330.609047	-1330.573995	-1330.672148	-1330.474507	-	-998.79
TS2d	-1331.155106	-1330.604970	-1330.570013	-1330.667630	-1330.470106	-	-1198.35
TS4	-1331.112566	-1330.563623	-1330.527694	-1330.628846	-1330.431573	-	-299.96
TS4'	-1331.187817	-1330.637834	-1330.602142	-1330.702613	-1330.502050	-	-493.46
TS4a	-1331.190121	-1330.639182	-1330.603831	-1330.703025	-1330.503381	-	-280.74

[a]Optimized at the B3LYP-D3/SDD-6-31G(d)/gas level of theory.
[b]Single point energies at the M06/SDD-6-311+G(d,p)/SMD(toluene) level of theory.
[c]Single point energies at the DLPNO-CCSD(T)/def2-TZVP/SMD(toluene) level of theory.

NEB Shows the Kinetic Barrier for Formation of Zr-bound Formic Acid

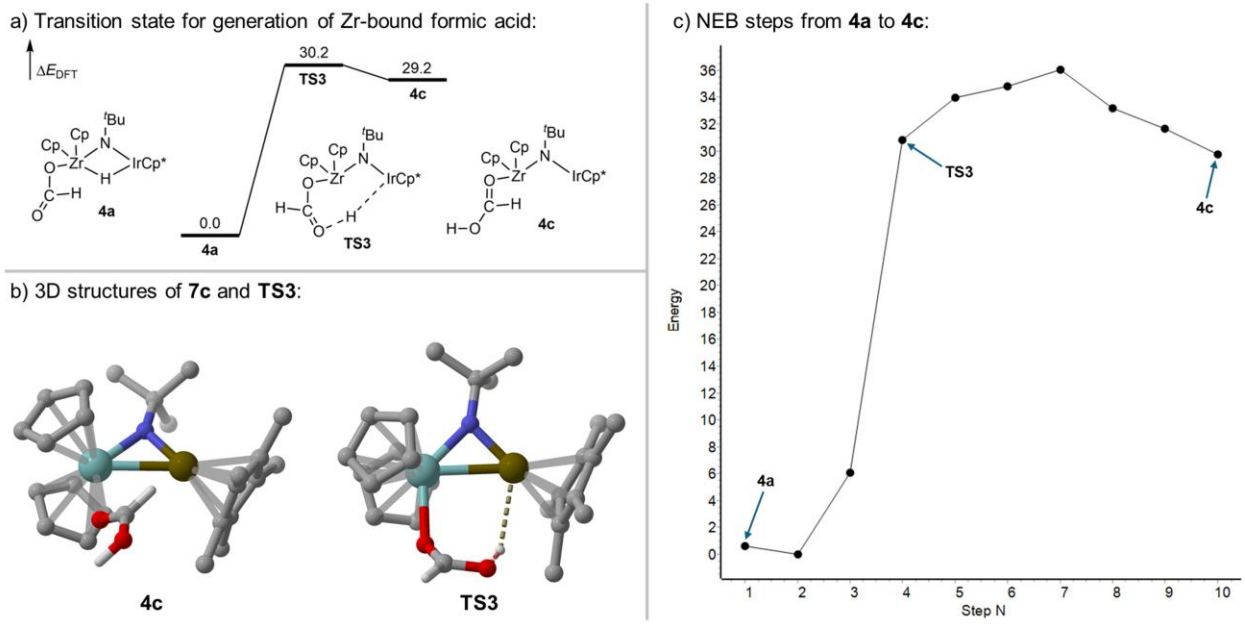

Figure S1. a) Intermediates and transition state energies from nudged elastic band (NEB) calculated at the B3LYP-D3/def2-SVP/gas level of theory using ORCA 6.0. The starting and endpoint geometries (i.e.; **4a** and **4c**) were optimized at the B3LYP-D3/SDD-6-31G(d)/gas level of theory using Gaussian 16. b) Optimized 3D structures of **4c** and **TS3**. c) Each step of the NEB calculation with their relative electronic energies. The barrier shown after **TS3** is the kinetic barrier to rotate the formic acid to the stationary point **4c** with the hydrogen facing away from the Iridium. All energies shown are electronic energies in kcal/mol.

NEB Shows H_2 Dissociation from Zr and Ir is Favorable

H_2 coordination to **3** at either Ir or Zr is highly unfavorable. To demonstrate this, nudged elastic band (NEB) calculations were run from the optimized frozen bond H_2-coordinated structures (M-H = 1.71 Å) to the fully optimized dissociated structures (Figure S2). The NEB pathway was uphill by 46.5 kcal/mol for coordination to Zr. Similarly, coordination of H_2 with Ir was thermodynamically disfavored by 13.1 kcal/mol.

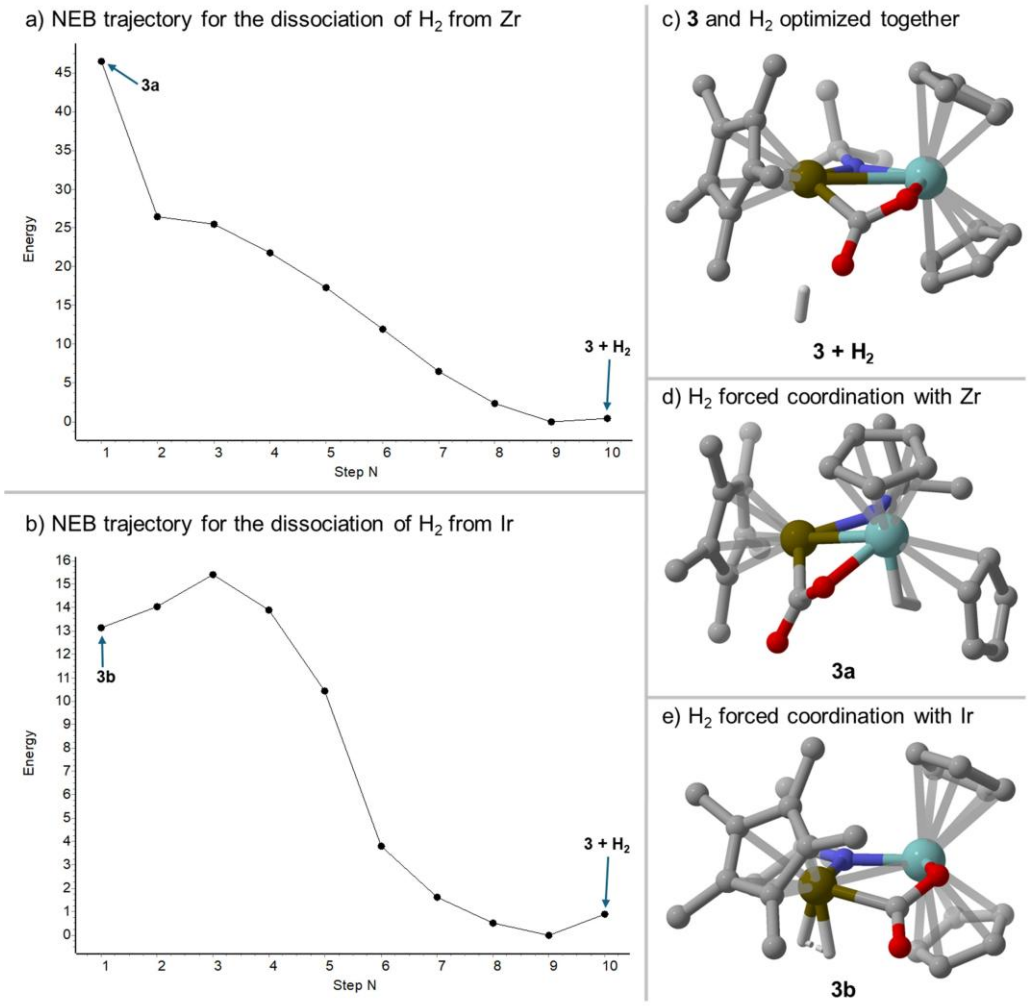

Figure S2. Nudged elastic band (NEB) pathways were calculated for H_2 dissociation from both zirconium and iridium (a and b, respectively), calculated at the B3LYP-D3/def2-SVP/gas level of theory using ORCA 6.0. The starting and endpoint geometries (i.e.; **3a**, **3b**, and **3 + H_2**) were optimized at the B3LYP-D3/SDD-6-31G(d)/gas level of theory using Gaussian 16. Both **3a** and **3b** were optimized with M-H coordinates frozen at 1.71 Å for one of the hydrogen atoms; spontaneous dissociation occurs if no bonds are frozen. All energies shown are electronic energies in kcal/mol.

H_2 Insertion into Zr-N, Zr-O, N-Ir and C-Ir Bonds is Kinetically Unfavorable

We examined transition states for H_2 1,2-addition across the four metal-main group atom bonds: N-Ir (**TS2a**), C-Ir (**TS2b**), Zr-N (**TS2c**), and Zr-O (**TS2d**) bonds (Figure S3). The free energy barriers of **TS2b**, **TS2c** and **TS2d** are above 30 kcal/mol which makes these H_2 additions virtually inaccessible at room temperature and therefore there would be no reactivity at room temperature. For the original **TS2**, the Ir-H bond distance is 1.64 Å and the Zr-H bond distance is 1.91 Å. However, in that complex H_2 is already bound to the Zr-Ir complex; the analogous transition state from CO_2-bound complex **3** is **TS2b**, which has a Ir-H bond distance of 2.12 Å, indicating a weaker M-H interaction and requires the breaking of the Ir-C bond. This corresponds to a much larger inaccessible barrier of 37.6 kcal/mol.

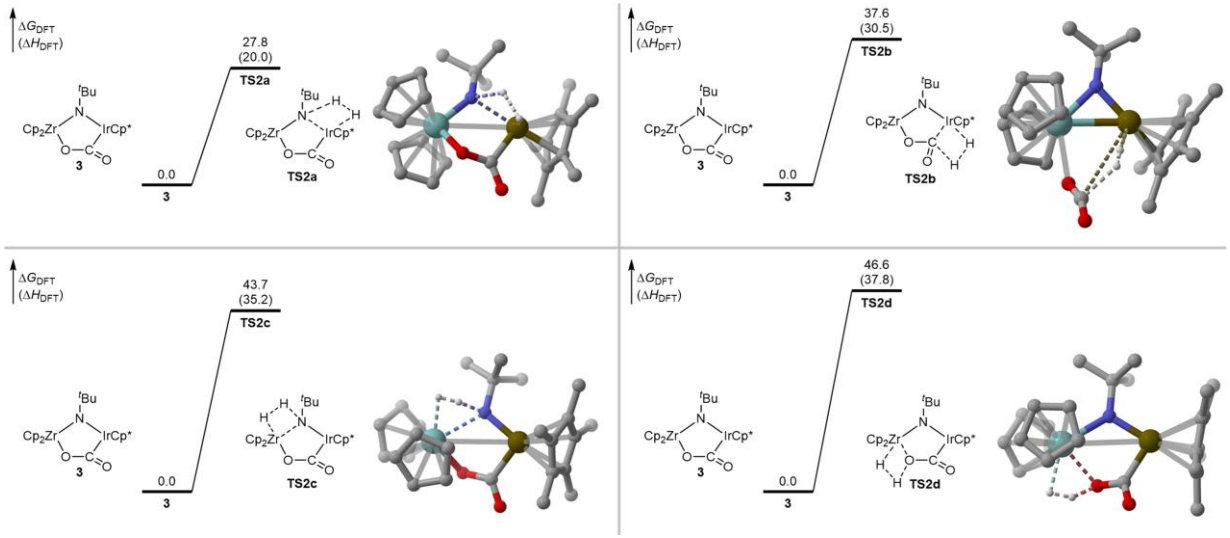

Figure S3. Each quadrant shows the transition state structure and free energy barrier for the insertion of H_2 into one of 4 bonds: N-Ir (top left), C-Ir (top right), Zr-N (bottom left), and Zr-O (bottom right). All energies shown are in kcal/mol.

QTAIM, ESM, Charge, and Orbital Analysis of 1

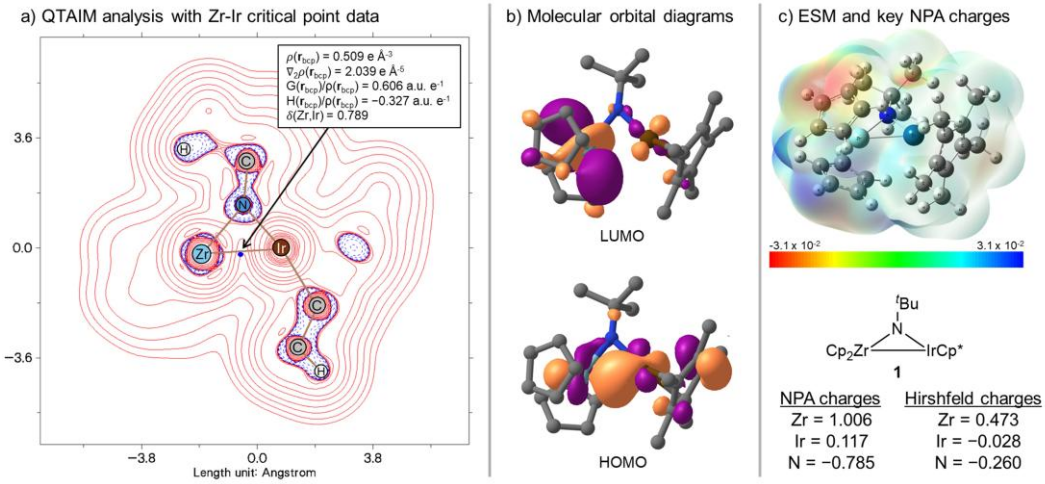

Figure S4. (a) QTAIM analysis of complex **1** showing the details of the Zr-Ir bond critical point, (b) highest occupied and lowest unoccupied molecular orbitals, and (c) electrostatic potential map and selected NPA charges.

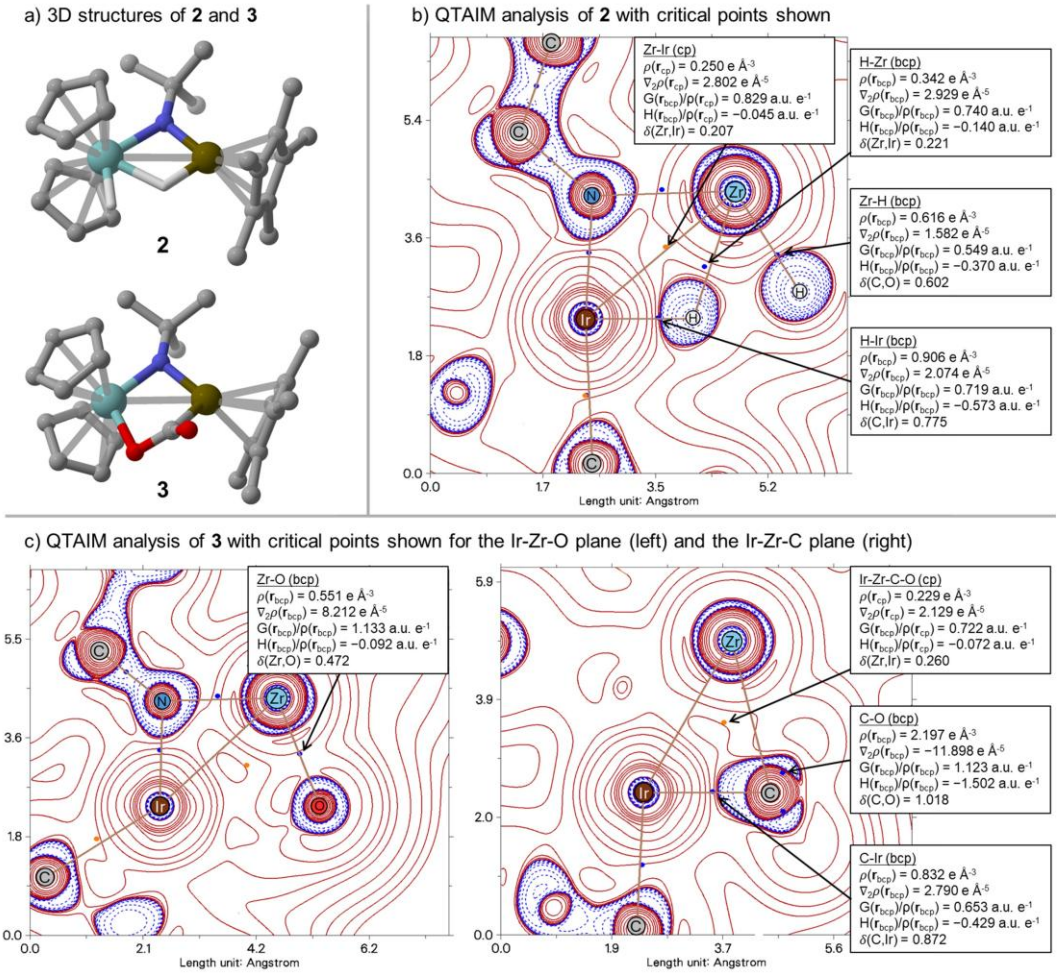

Figure S5. (a) 3D structure of **2** and **3** for comparison. (b) QTAIM analysis of complex **2** showing the details of the Zr-Ir critical point, and key bond critical points. (c) QTAIM analysis of complex **3** showing the details of the critical point between Ir, Zr, C, and O and key bond critical points. Since the carbon and oxygen are on different planes, both places were plotted separately.

Possible Alternative Geometries for CO_2 and H_2

Alternative geometries were tested for CO_2 and H_2 coordination as well as alternative CO_2 addition transition states. These are disfavored due to the additional distortion of the Cp* ligand or the breaking of favorable interactions compared to the most favorable pathway.

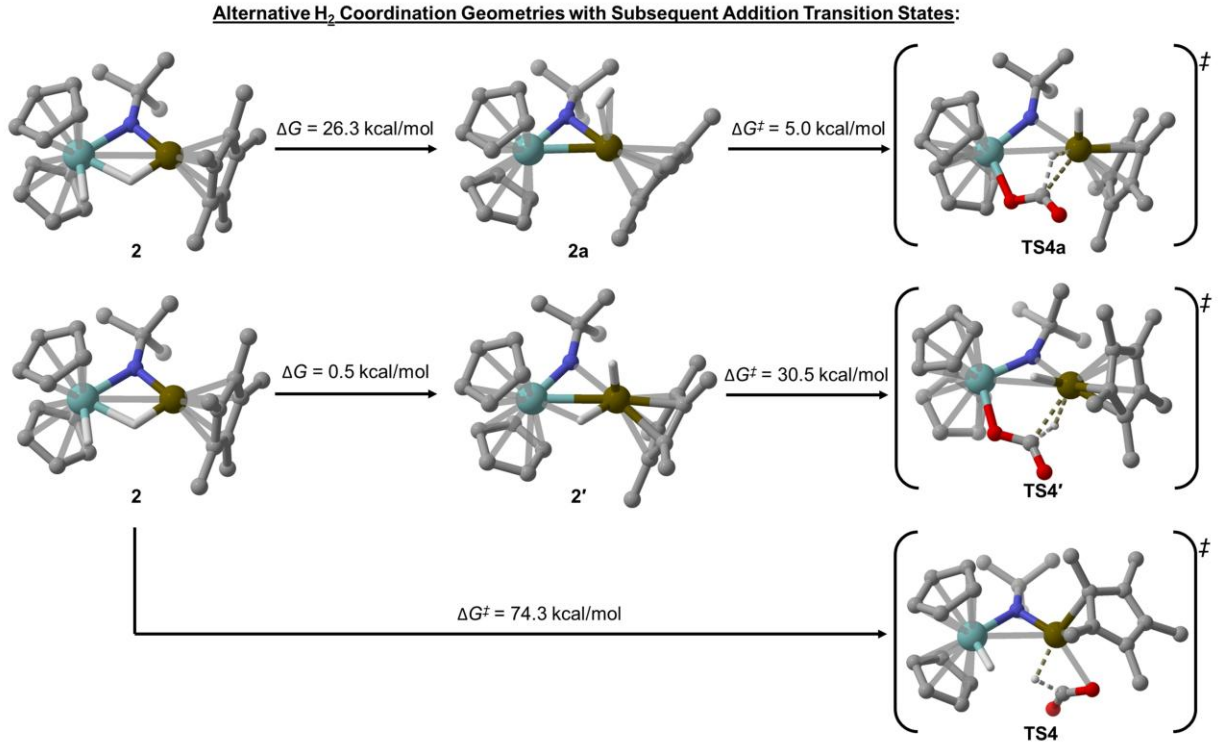

Figure S6. Successfully optimized alternative H_2 coordination geometries and their subsequent CO_2 addition transition states calculated at the M06/6-311+G(d,p)-SDD/SMD(toluene)//B3LYP-D3/6-31G(d)-SDD level of theory.

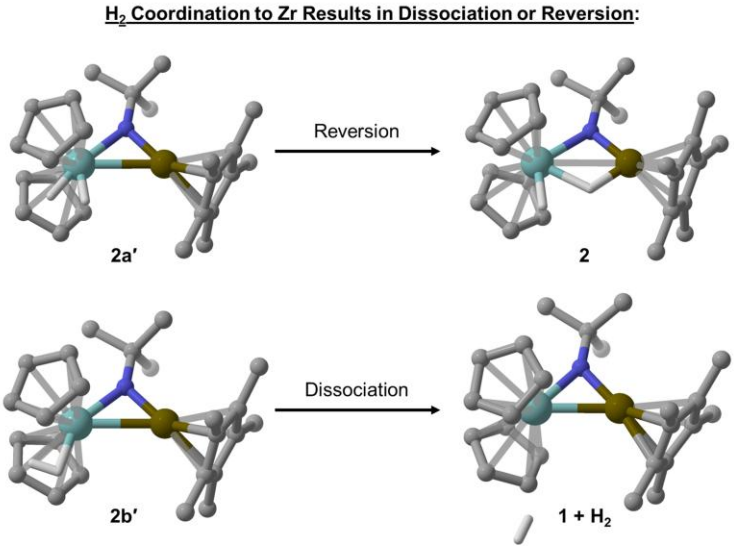

Figure S7. Attempts to locate alternative H_2 coordination geometries optimized at the B3LYP-D3/6-31G(d)-SDD level of theory.

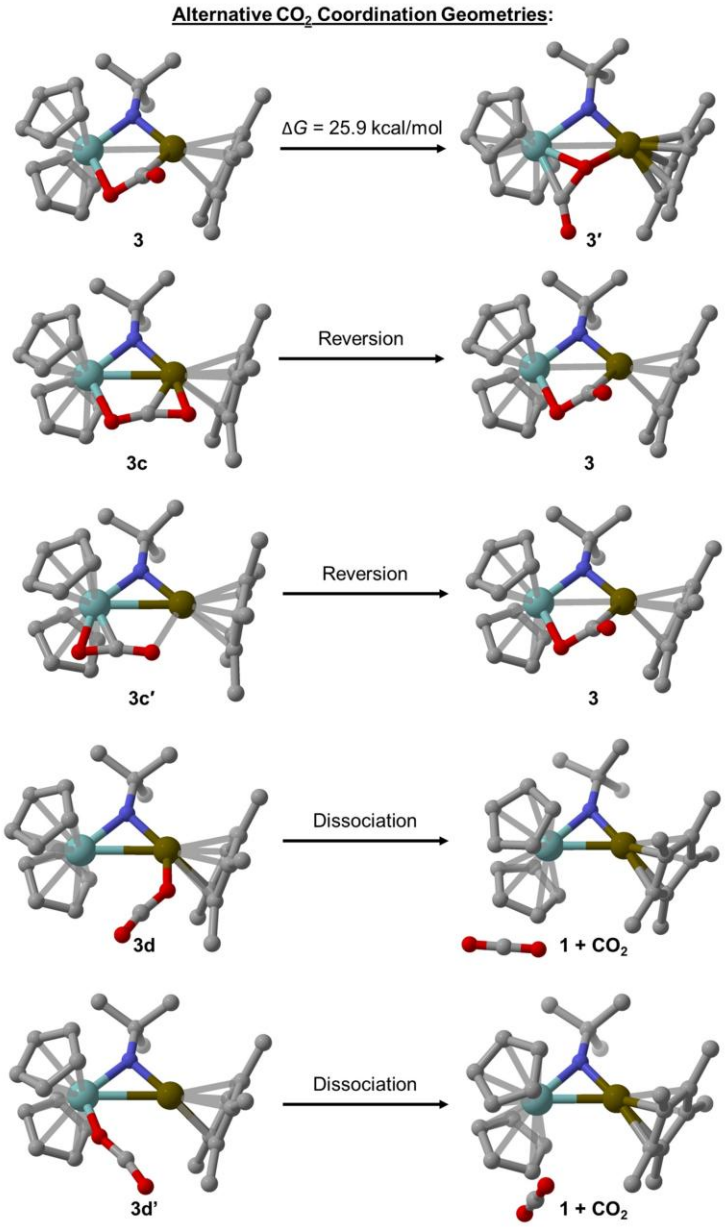

Figure S8. Attempts to locate alternative CO_2 coordination geometries optimized at the B3LYP-D3/6-31G(d)-SDD level of theory. Single point energy: M06/6-311+G(d,p)-SDD/SMD(toluene).

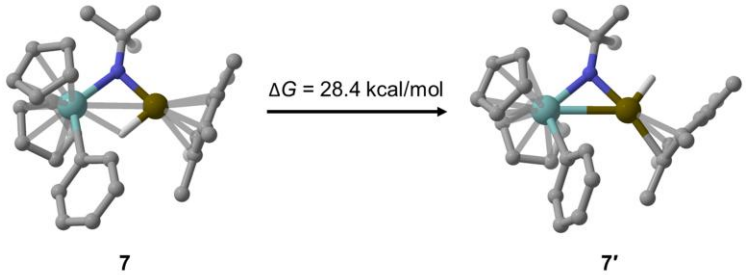

Figure S9. Successfully optimized broken hydrogen bridge coordination geometry for complex **7** calculated at the M06/6-311+G(d,p)-SDD/SMD(toluene)//B3LYP-D3/6-31G(d)-SDD level of theory. Breaking the bridging hydrogen interaction is significantly energetically disfavored.

Geometry Optimization with B3LYP-D3 vs. MN15-L

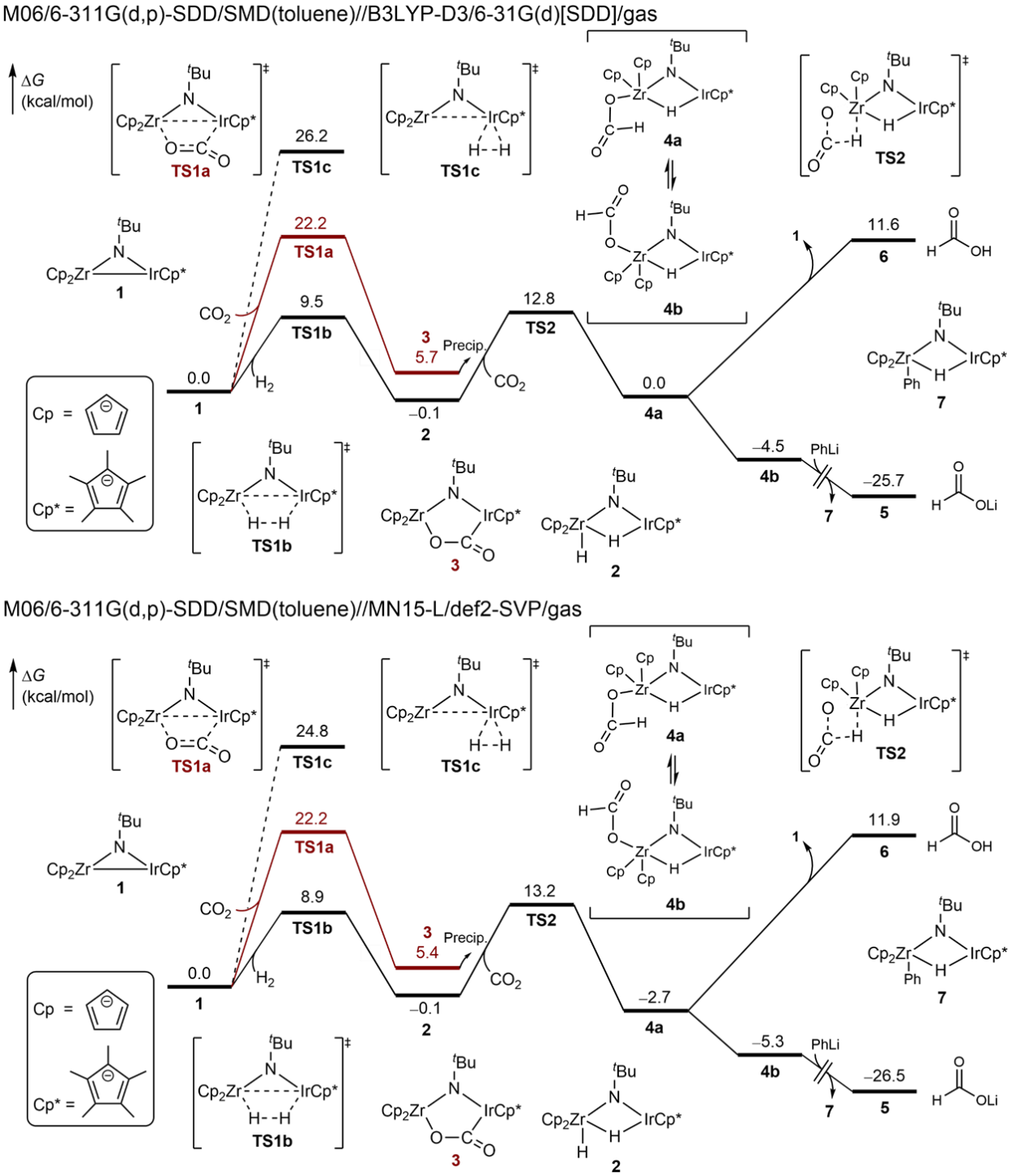

Figure S10. Geometry optimization at the B3LYP-D3/6-31G(d)-SDD level of theory versus optimization at the MN15-L/def2-SVP level of theory with single point energy calculations at the M06/6-311+G(d,p)-SDD/SMD(toluene) level of theory.

Table S2. Computed energies and imaginary frequencies of MN15-L/def2-SVP optimized structures.

Complex[a]	SCF	ZPE	Enthalpy	Free energy	SP-Free energy[b]	Freq.
CO_2	-188.256954	-188.244904	-188.241344	-188.266258	-188.559117	-
H_2	-1.162459	-1.152293	-1.148988	-1.163822	-1.170011	-
PhLi	-238.725734	-238.636470	-238.629596	-238.666131	-239.026703	-
1	-1139.000524	-1138.484417	-1138.452274	-1138.544121	-1140.772685	-
2	-1140.189668	-1139.656022	-1139.623963	-1139.714865	-1141.962552	-
3	-1327.299458	-1326.766344	-1326.732677	-1326.825251	-1329.350301	-
4a	-1328.479629	-1327.927964	-1327.892490	-1327.990373	-1330.549691	-
4b	-1328.486885	-1327.934970	-1327.899693	-1327.997310	-1330.554145	-
5	-196.417535	-196.393260	-196.388427	-196.418682	-196.737565	-
6	-189.414675	-189.380087	-189.376010	-189.404156	-189.731316	-
7	-1370.839671	-1370.220710	-1370.184081	-1370.283204	-1372.883100	-
TS1a	-1327.266799	-1326.735501	-1326.701444	-1326.794897	-1329.321225	-124.66
TS1b	-1140.167507	-1139.637958	-1139.604491	-1139.697278	-1141.943660	-72.29
TS2	-1328.450828	-1327.904016	-1327.869060	-1327.965782	-1330.520030	-428.69

[a]Optimized at the MN15-L/def2-SVP/gas level of theory.
[b]Single point energies at the M06/SDD-6-311+G(d,p)/SMD(toluene) level of theory.

Reaction Rates at Various Temperatures

Bergman and coworkers conduct the reaction of H_2 and CO_2 with **1** starting from -196 °C and raising the temperature to -30 °C. They also note that the CO_2 bound complex (**3**) is unstable at room temperature while in solution but is stable as a solid. These rates are calculated using our calculated Gibbs free energy values, and are consistent with the experimental results.

Table S3. Select reaction rates for the addition and loss of H_2 and CO_2 from **1** at different reaction temperatures. All energies are in kcal/mol and are taken from the reported energy surface (Figure 2).

Rates @ -100 °C	Temp (K)	Gibbs E	k	t1/2 (sec)	t1/2 (min)	t1/2 (h)	t1/2 (days)
Addition of H2 (**1** -> **2**)	173	12.4	7.8E-04	8.9E+02	14.80	0.25	0.01
Loss of H2 (**2** -> **1**)	173	18.4	2.1E-11	3.4E+10	5.62E+08	9.37E+06	3.90E+05
Addition of CO2 (**2** -> **4a**)	173	12.7	3.3E-04	2.13E+03	35.43	0.59	0.02

Rates @ -30 °C	Temp (K)	Gibbs E	k	t1/2 (sec)	t1/2 (min)	t1/2 (h)	t1/2 (days)
Addition of H2 (**1** -> **2**)	243	12.4	3.6E+01	1.9E-02	0.00	0.00	0.00
Loss of H2 (**2** -> **1**)	243	18.4	1.4E-04	4.8E+03	8.06E+01	1.34E+00	5.60E-02
Addition of CO2 (**2** -> **4a**)	243	12.7	1.9E+01	3.62E-02	0.00	0.00	0.00

Rates @ 25 °C	Temp (K)	Gibbs E	k	t1/2 (sec)	t1/2 (min)	t1/2 (h)	t1/2 (days)
Loss of CO2 (**3** -> **1**)	298.15	27	1.0E-07	6.9E+06	1.15E+05	1.92E+03	79.84

NEB Shows that 2 and 4a are Connected Through TS2

Figure S11 shows the NEB calculated pathway for reaction of the Zr-H intermediate with CO_2.

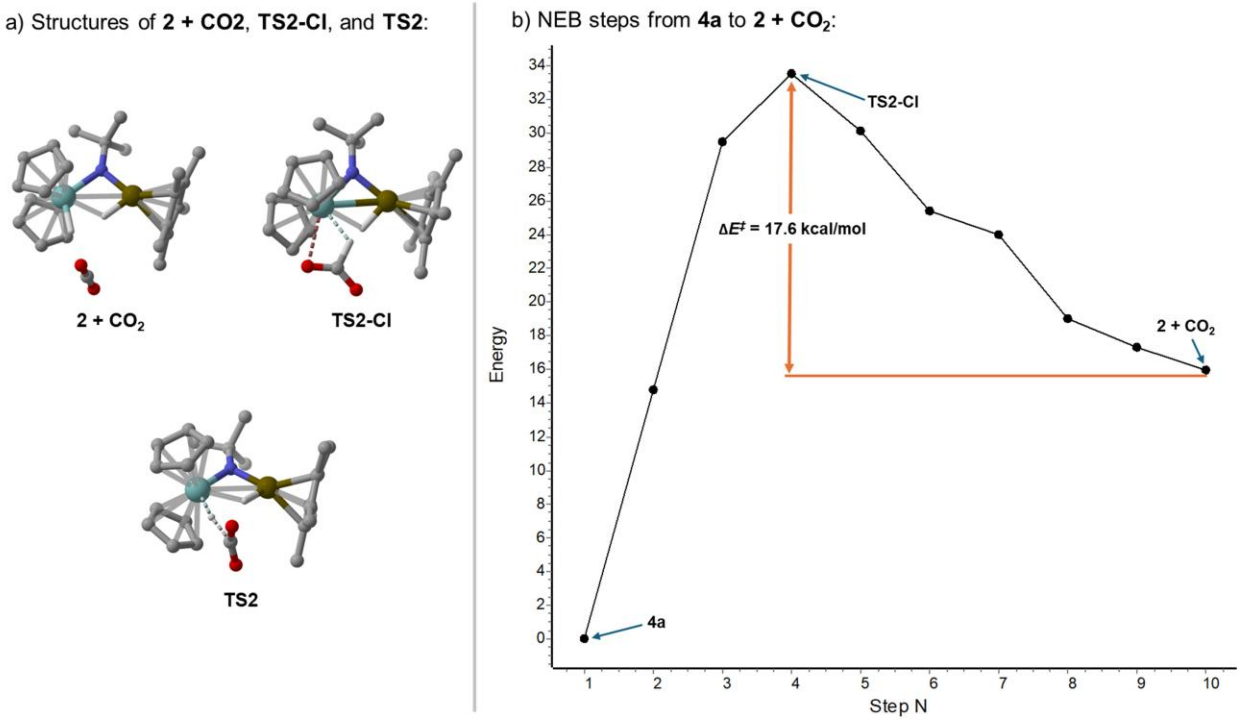

Figure S11. (a) The structures of **2 + CO_2** and **TS2-CI** as located via NEB calculation. The NEB located transition state **TS2-CI** corresponds to the breaking of the Zr-H bond and the formation of the O-Zr bond, with the C-H bond being nearly fully formed (1.2 Å). (b) NEB trajectories from **4a** to **2 + CO_2** with the electronic energy barrier shown. Nudged elastic band (NEB) trajectories were calculated at the B3LYP(g)-D3/def2-SVP/gas level of theory using ORCA 6.0. The starting point geometry (i.e.; **4a**) was optimized at the B3LYP-D3/SDD-6-31G(d)/gas level of theory using Gaussian 16 and the end point geometry (i.e.; **2 + CO_2**) was optimized at the B3LYP(g)-D3/def2-SVP/gas level of theory in ORCA 6.0 starting from a manually displaced **TS2** geometry.

^{t}Bu and Cp* Ligand Impact on Reactivity

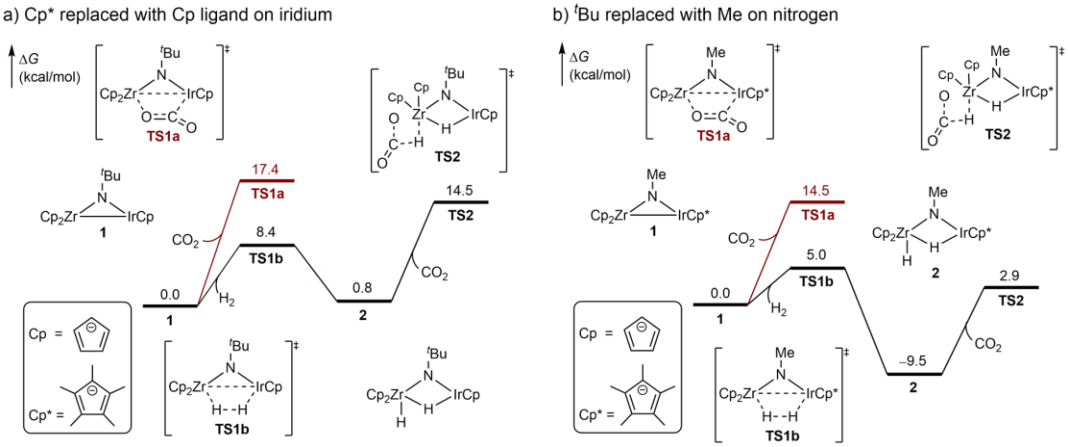

Figure S12. Energy surfaces showing (a) ^{t}Bu replaced with Me and (b) Cp* replaced with Cp. There is a noticeable effect on reactivity, likely due to dispersion and steric effects; this effect could reduce

selectivity between complexes **2** and **3**. Theory level: M06/6-311G(d,p)-SDD/SMD(PhMe)//B3LYP-D3/6-31G(d)-SDD

References

(1) Neese, F. The ORCA program system. *WIREs Computational Molecular Science* **2012**, *2* (1), 73-78. DOI: https://doi.org/10.1002/wcms.81.

(2) (a) A. D. Becke, *The Journal of Chemical Physics*, 1993, **98**, 5648-5652. (b) S. Grimme, J. Antony, S. Ehrlich and H. Krieg, *The Journal of Chemical Physics*, 2010, **132**.

(3) F. Weigend and R. Ahlrichs, *Physical Chemistry Chemical Physics*, 2005, **7**, 3297-3305.

(4) M. J. Frisch, G. W. Trucks, H. B. Schlegel, G. E. Scuseria, M. A. Robb, J. R. Cheeseman, G. Scalmani, V. Barone, G. A. Petersson, H. Nakatsuji, X. Li, M. Caricato, A. V. Marenich, J. Bloino, B. G. Janesko, R. Gomperts, B. Mennucci, H. P. Hratchian, J. V. Ortiz, A. F. Izmaylov, J. L. Sonnenberg, Williams, F. Ding, F. Lipparini, F. Egidi, J. Goings, B. Peng, A. Petrone, T. Henderson, D. Ranasinghe, V. G. Zakrzewski, J. Gao, N. Rega, G. Zheng, W. Liang, M. Hada, M. Ehara, K. Toyota, R. Fukuda, J. Hasegawa, M. Ishida, T. Nakajima, Y. Honda, O. Kitao, H. Nakai, T. Vreven, K. Throssell, J. A. Montgomery Jr., J. E. Peralta, F. Ogliaro, M. J. Bearpark, J. J. Heyd, E. N. Brothers, K. N. Kudin, V. N. Staroverov, T. A. Keith, R. Kobayashi, J. Normand, K. Raghavachari, A. P. Rendell, J. C. Burant, S. S. Iyengar, J. Tomasi, M. Cossi, J. M. Millam, M. Klene, C. Adamo, R. Cammi, J. W. Ochterski, R. L. Martin, K. Morokuma, O. Farkas, J. B. Foresman and D. J. Fox, *Journal*, 2016.

(5) (a) T. H. Dunning and P. J. Hay, in *Methods of Electronic Structure Theory*, ed. H. F. Schaefer, Springer US, Boston, MA, 1977, DOI: 10.1007/978-1-4757-0887-5_1, pp. 1-27. (b) W. J. Hehre, R. Ditchfield and J. A. Pople, *The Journal of Chemical Physics*, 1972, **56**, 2257-2261. (c) R. Ditchfield, W. J. Hehre and J. A. Pople, *The Journal of Chemical Physics*, 1971, **54**, 724-728. (d) P. C. Hariharan and J. A. Pople, *Theoretica chimica acta*, 1973, **28**, 213-222.